CHEMISTRY
A EUROPEAN JOURNAL

DOI: 10.1002/chem.200902627

Spatially Controllable DNA Condensation by a Water-Soluble Supramolecular Hybrid of Single-Walled Carbon Nanotubes and β-Cyclodextrin-Tethered Ruthenium Complexes

Miao Yu,[a] Sheng-Zhen Zu,[b] Yong Chen,[a] Yu-Ping Liu,[c] Bao-Hang Han,*[b] and Yu Liu*[a]

Dedicated to Professor Yoshihisa Inoue on the occasion of his 60th birthday

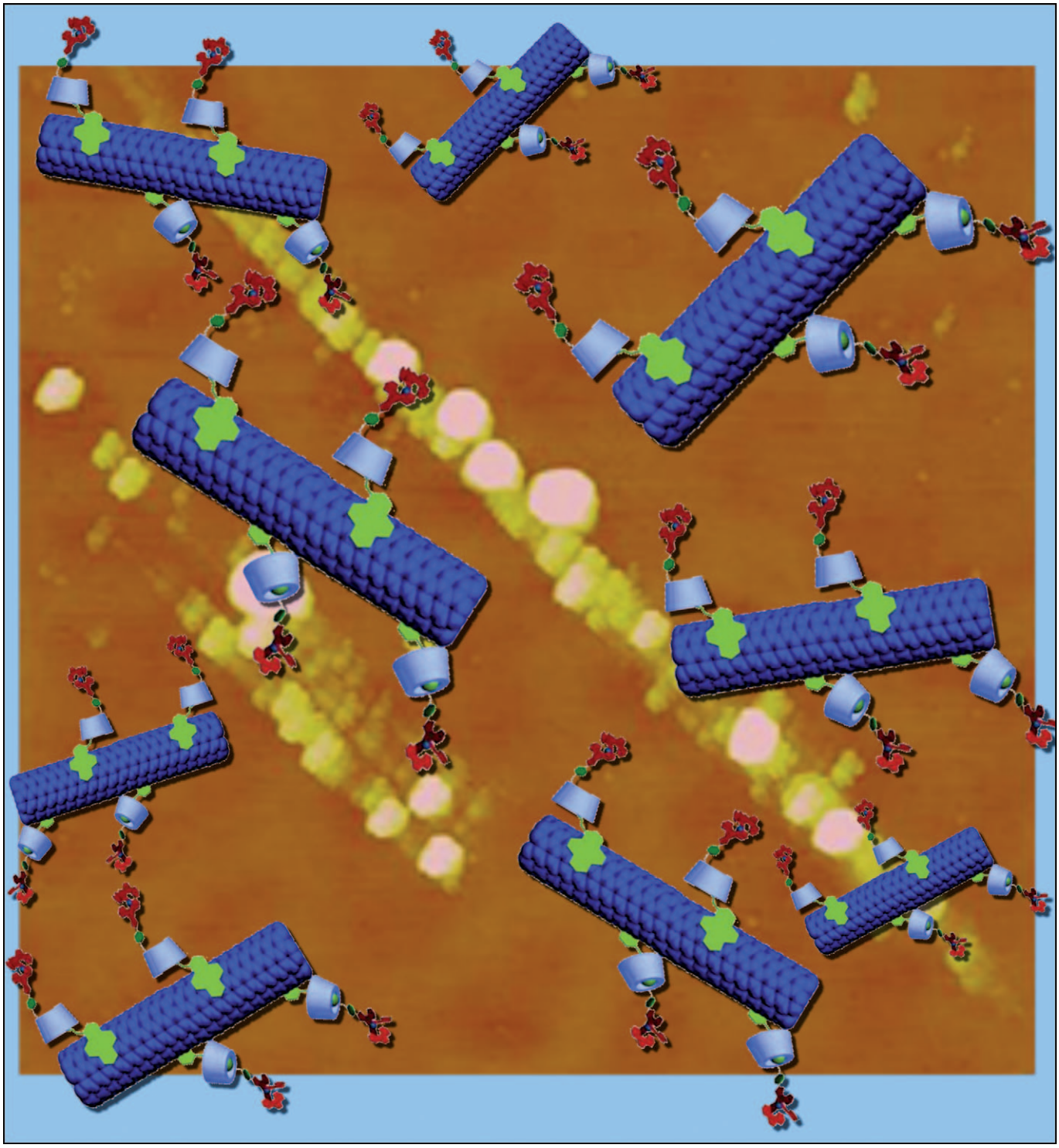

Abstract: A supramolecular hybrid is prepared by the supramolecular surface modification of single-walled carbon nanotube (SWCNT) with cationic β-cyclodextrin-tethered ruthenium complexes through a spacer molecule that contains both an adamantane and a pyrene moiety. By employing the supramolecular hybrid, spatially controllable DNA condensation along the SWCNT skeleton is achieved by anchoring cationic ruthenium complexes on the surface. Furthermore, because of the unique physiological properties of SWCNTs, the cationic supramolecular hybrid can be used as a nonviral gene delivery system with the ruthenium complexes as a fluorescent probe to monitor uptake of DNA by cells.

Keywords: cyclodextrins · DNA · ruthenium · nanotubes · single-walled carbon nanotubes

Introduction

In the past years, DNA delivery systems have found many applications in gene therapy as a method of treating genetic disorders.[1] Nonviral DNA delivery systems have attracted much attention for their relative safety and ease of application.[2] Controllable DNA condensation will be significantly helpful for gene delivery systems.[3] Reversible photoswitched DNA condensation employing azobenzene-containing light-responsive cationic surfactants have been reported.[4] In the meantime, a spatially controllable DNA condensation system will be also crucial for future applications. Recently, we have prepared a water-soluble β-cyclodextrin (β-CD)-containing ruthenium complex ([Ru(phen)$_2$(β-CD-hophen)]Cl$_2$, signified as β-CD-RC, phen = 1,10-phenanthroline, β-CD-hophen = 2-(4′-hydroxyphenyl)-imidazo[*f*]-1,10-phenanthroline-modified β-CD, see Scheme 1) and found that it is able to induce DNA aggregation, resulting in submicrometer DNA toroids and transfection into 293T cells.[5]

Because carbon nanotubes (CNTs) possess the properties of cell-permeability without imparting toxicity,[6] there are an enormous number of ongoing explorations into CNT use in biological and medical application fields,[7] such as an agent for protein and DNA transport, nanomedical functional excipient, or intracellular transport of biologically active molecules for gene therapy.[8] We have employed adamantane-modified pyrene supramolecular assemblies on multi-walled carbon nanotubes (MWCNT) in aqueous solution to explore its DNA condensation capacity and found that MWCNT could enhance DNA condensing efficiency of cationic polymers.[9] Prato and co-workers investigated the condensation of plasmid DNA by cationic covalently functionalized SWCNTs and MWCNTs and explored their potential as gene-transfer agents.[10] Lee and Johnson have investigated the interaction between DNA with positively charged SWCNTs.[11]

As a type of well-defined CNT, SWCNTs possess some unique properties compared to MWCNTs. Therefore, SWCNTs have been investigated intensively and systematically. As an efficient and less-destructive approach to improve the solubility and dispersibility of SWCNTs, noncovalent surface modification has been extensively employed through π–π stacking interactions, van der Waals interactions, and/or hydrophobic interactions between the surface of CNT and either aromatic compounds, nucleic acids, polymers, ss-DNA, or host–guest complexes.[12] To the best of our knowledge, DNA condensation by functionalized CNTs or CNT hybrids has not given well-structured and controlled morphology to date. Recently, we reported a supramolecular surface modification of SWCNTs by the inclusion complex of methylated β-cyclodextrin (β-MCD) with adamantane derivatives (Py-Ad) that are tethered with a pyrene moiety.[13] The formation of the SWCNT–Py-Ad–β-MCD supramolecular hybrid results in the water-solubilization of SWCNTs, in which the SWCNT is the core, and the adamantane–cyclodextrin complexes are the water-soluble shell/corona. If we replace the β-MCD with β-CD-tethered ruthenium complex ([Ru(phen)$_2$(β-CD-hophen)]Cl$_2$, β-CD-RC), we obtain an aqueous solution of supramolecular SWCNT–Py-Ad–β-CD-RC (**1**), in which a layer of cationic ruthenium complexes are anchored on the surface of the supramolecular hybrid (Scheme 1). By employing the supramolecular hybrid system, we can achieve spatially controllable DNA condensation along the SWCNTs. In this article, we present this attempt and report the hybrid–DNA complex uptake by cells.

Results and Discussion

On the basis of our recent report,[13] the aqueous solution of **1** was prepared with β-CD-containing ruthenium complexes by using a modified procedure from the literature.[14] We mixed and finely ground the solid sample to improve the stability of the aqueous solution, and the final product was dialyzed with ultrapure water to ensure the complete removal of excess β-CD-RC and Py-Ad.

[a] M. Yu, Dr. Y. Chen, Prof. Dr. Y. Liu
Department of Chemistry
State Key Laboratory of Elemento-Organic Chemistry
Nankai University, Tianjin, 300071 (P. R. China)
Fax: (+86) 22-2350-3625
E-mail: yuliu@nankai.edu.cn

[b] Dr. S.-Z. Zu, Prof. Dr. B.-H. Han
National Center for Nanoscience and Technology
Beijing 100190 (P. R. China)
Fax: (+86) 10-8254-5576
E-mail: hanbh@nanoctr.cn

[c] Dr. Y.-P. Liu
Research Center for Analytic Sciences
Nankai University, Tianjin 300071 (P. R. China)

Supporting information for this article is available on the WWW under http://dx.doi.org/10.1002/chem.200902627.

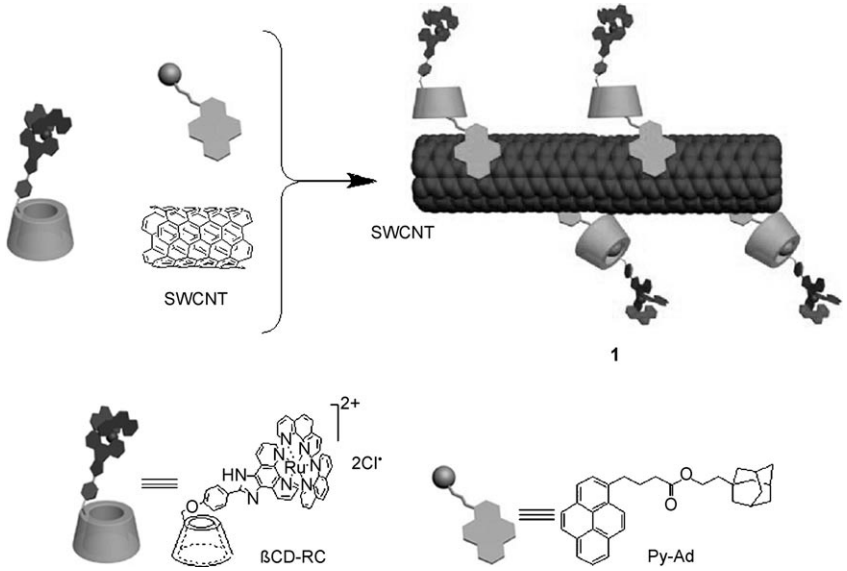

Scheme 1. Preparation route to the SWCNT–Py-Ad–β-CD-RC supramolecular hybrid (**1**).

Systematic investigations have been performed to elucidate the interactions among β-CD-RC, Py-Ad, and SWCNT in solution. The fluorescence emission at 360–430 nm of Py-Ad in DMF solution decreases gradually with stepwise addition of a SWCNT solution at 25 °C (Supporting Information, Figure S1), which indicates that a π–π stacking interaction exists between Py-Ad and the surface of SWCNT. Meanwhile, the fluorescence emission of aqueous β-CD-RC solution slightly decreases upon the addition of Py-Ad solution (Supporting Information, Figure S2); this suggests that an inclusion complex forms between the adamantyl moiety of Py-Ad and the cyclodextrin cavity upon the decrease of the microenvironmental hydrophobicity and/or steric deshielding around the fluorophore (the Ru-complex unit in β-CD-RC).[15] At the same time, it can also be attributed to interactions such as electron (charge) transfer between the pyrene moiety and fluorescent ruthenium complex.[15a] Furthermore, the fluorescence intensity of β-CD-RC at 600 nm does not show any change upon addition of SWCNT in aqueous solution (Supporting Information, Figure S3), which indicates that there is no detectable interaction between the ruthenium complex and SWCNT in aqueous solution in the absence of the Py-Ad segment. Under the fluorescence experimental conditions described above, the competitive light absorbance of SWCNT and Py-Ad can be ignored because they are too low to be determined.

From the UV/Vis spectrum of an aqueous solution of **1** (Figure 1), both the characteristic absorbance peak at 460 nm for β-CD-RC and the characteristic absorbance peaks at 330 and 340 nm for Py-Ad are observed; this indicates the co-presence of β-CD-RC and Py-Ad in the aqueous supramolecular hybrid solution. The concentration of aqueous **1** (300.0 ng μL^{-1}) is approximately 60 μM as calculated from the β-CD-RC extinction coefficient in aqueous solution that was obtained from the working plot (Supporting Information, Figure S4); this was determined by measuring the UV/Vis absorbance at 460 nm at various concentrations (extinction coefficient ε of β-CD-RC obtained as $(6.92\pm0.04)\times10^3$ L mol^{-1} cm^{-1}).

Furthermore, we notice that the fluorescence intensity of β-CD-RC in the aqueous solution of **1** decreased remarkably compared with that in aqueous β-CD-RC (Figure 2); this indicates the appearance of a photo-induced charge-transfer process from the SWCNT–Py-Ad moiety to the β-CD-RC in the supramolecular hybrid.[15a]

The Vis/NIR spectrum of aqueous **1** is shown in Figure S5 (Supporting Information). In the range of 600–1300 nm, the

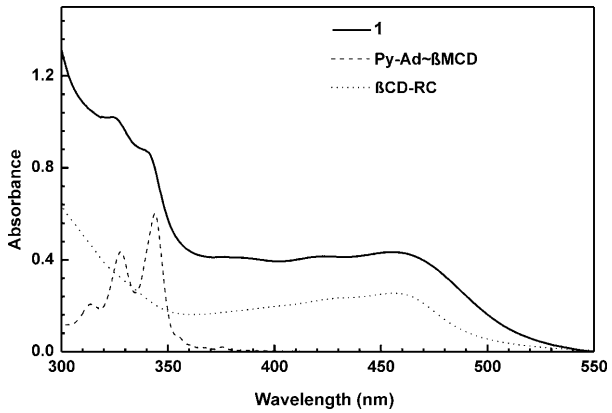

Figure 1. UV/Vis spectrum of aqueous **1** (solid line, [hybrid] = 300 ng μL^{-1}, that is, ≈[β-CD-RC] = 60 μM), Py-Ad–β-MCD (dash line), and β-CD-RC (dot line, 50 μM) solutions (25 °C).

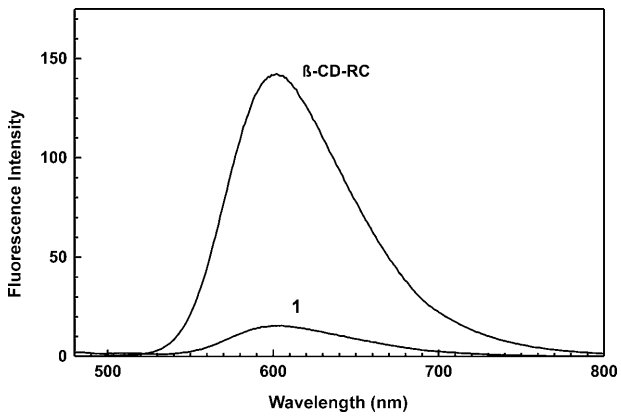

Figure 2. Fluorescence spectra of β-CD-RC (2.0 μM) and **1** ([hybrid] = 10.0 ng μL^{-1}, that is, [β-CD-RC] = 2.0 μM) excited at 460 nm (25 °C).

typical SWCNT van Hove singularities indicate highly dispersed individual SWCNTs.[16]

The disorder-induced band (*D*-band) and tangential graphite mode (*G*-band) of SWCNT are found at 1320 and 1590 cm^{-1} in the room-temperature Raman spectra (Supporting Information, Figure S6). The relative intensity of *D*-band in the Raman spectra, which correlates with defects in SWCNT structure,[17] has no significant change owing to the treatment. From the above phenomena, we can conclude the treatment method has not damaged the SWCNT electronic structure.[18]

We have also obtained both qualitative and quantitative evidence for a supramolecular hybrid (**1**) by using X-ray photoelectron spectroscopy (XPS).[19] As can be seen in Figure 3, the C1s spectrum of SWCNT can be typically divided into five components (284.5, 285.5, 286.9, 288.6, and

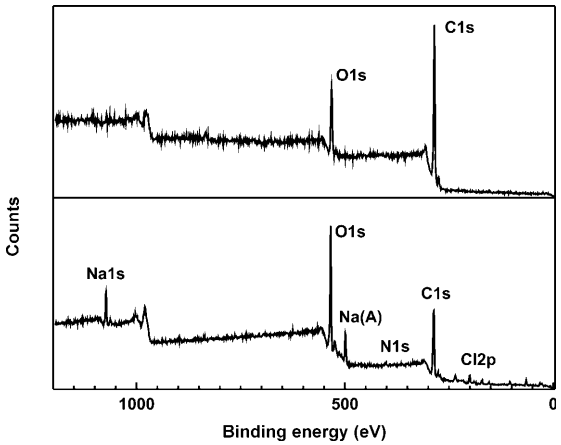

Figure 3. XPS survey spectra of SWCNT (upper) and **1** (lower).

291.4 eV), which are contributed by graphite-like carbon atoms, C–OR, C=O, COOH, and sp^2-hybridized carbon $\pi^* \leftarrow \pi$ shake-up, respectively.[20] In Figure S7 (Supporting Information), the corresponding peaks of the involved elements emerge in the XPS survey spectrum of **1**. The nitrogen and chlorine in β-CD-RC give related peaks at 400 and 200 eV, respectively. The sodium atom is introduced by a neutralization reaction between sodium hydroxide and carboxyl group of SWCNT in the hybrid preparation process. The appearance of multivalent ruthenium ions peaks at 281.1 and 282.0 eV close to the C1s spectrum demonstrates the formation of **1**.[20b] Furthermore, the C1s spectrum of the supramolecular hybrid consists of four components (284.6, 285.8, 287.0, and 289.0 eV). Comparing the C1s spectra of supramolecular hybrid and SWCNT (Supporting Information, Figure S7), we notice some differences, as follows: the sp^2-hybridized carbon $\pi^* \leftarrow \pi$ shake-up peak at 291 eV disappears in the C1s spectrum of the supramolecular hybrid, which indicates that SWCNT bundles have been dispersed by the noncovalent modification.[9] The COOR carbon peak at 289 eV becomes weaker for the addition of Py-Ad and β-CD-RC. The C–OR carbon peak at 285.8 eV becomes higher owing to high content of C–O in cyclodextrin moiety.

From the XPS data of **1** (elemental analysis: C%, 64.02; N%, 1.74), we can conclude that there are eight nitrogen atoms for every 295 carbon atoms. Considering that there are eight nitrogen atoms for every 117 carbon atoms in the Py-Ad–β-CD-RC complex, there can be only one Py-Ad–β-CD-RC moiety for every 178 SWCNT carbons (ca. 4.1 nm^2 of SWCNT surface). This also means that there is one mole of β-CD-RC in approximately 4638 g of supramolecular hybrid (that is, [hybrid] = 10.0 $ng\,\mu L^{-1}$ with [β-CD-RC] = 2.2 μM), which is smaller than the calculated value (ca. 5000 $g\,mol^{-1}$) through the β-CD-RC extinction coefficient considering there are some hydrated water molecules in the supramolecular hybrid. Then we can deduce that the possible structure of supramolecular hybrid as shown in the Scheme 1.

Direct information about **1** is revealed by the high-resolution transmission electron microscopy (HR-TEM) and atomic force microscopy (AFM). The supramolecular hybrid in aqueous solution is observed by HR-TEM (Supporting Information, Figure S8), and shows similar images to our former report.[13] AFM section analysis presents the diameter of SWCNT as approximately 0.9 nm and the height of the modified SWCNT domain as approximately 2.2 nm (Figure 4). The difference in their dimension is accordance with the thickness of two layers of cyclodextrin (ca. 0.7 nm).[21]

The condensation ability of **1** with pUC-19 plasmid DNA was investigated with agarose gel electrophoresis (GEP)

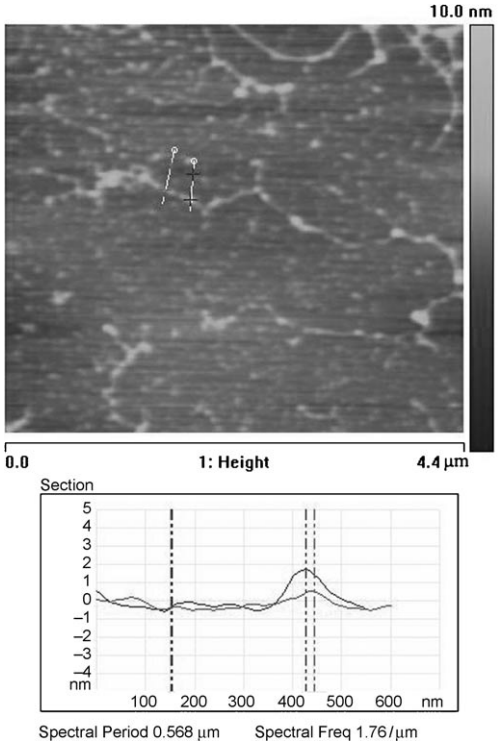

Figure 4. The AFM image of **1**.

analysis and atomic force microscope (AFM). Because the electrophoretic mobility of DNA decreases after condensation,[22] agarose gel electrophoresis analysis was used to investigate the condensation behavior of plasmid DNA pUC19 as a model DNA in the absence and presence of the supramolecular hybrid **1** by using ethidium bromide as a fluorescent tag, which is an intercalating agent for nucleic acids.[23] Figure 5 represents the gel mobility characterization

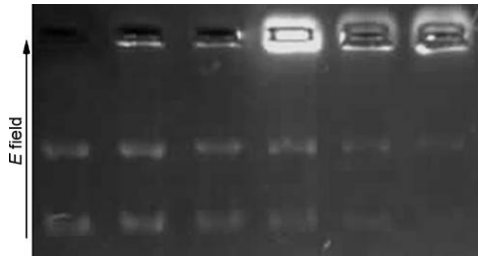

Figure 5. Agarose gel electrophoretogram of pUC19 plasmid DNA ([DNA] = 12.5 ng μL^{-1}) condensed with the supramolecular hybrid (**1**). From left to right: Lane 1, DNA only; lane 2–6, DNA + supramolecular hybrid ([hybrid] = 150, 250, 500, 1000, and 1250 ng μL^{-1}, i.e., [β-CD-RC] = 0.03, 0.05, 0.10, 0.20, and 0.25 mM). All samples are incubated at 25 °C in the dark for 1 h, 1 mM EDTA/10 mM Tris buffer, pH 8.0.

of DNA condensed by the supramolecular hybrid. Lanes 2–6 clearly indicate that plasmid DNA is condensed by the supramolecular hybrid because DNA can not migrate out of the gel well upon the addition of **1**. The free plasmid DNA bands become weaker because of the condensation of DNA with **1** from lane 2–6. We even notice that the bright band in the gel well shows some migration to the negative electrode with increasing ratios of supramolecular hybrid.

We also employed AFM in tapping mode to get detailed insight into the DNA structural change in the presence of the supramolecular hybrid **1**. Generally, the plasmid DNA exists as a mixture of circular supercoiled (CS) DNA and open circular (OC) DNA.[24] As shown in Figure 6a, most of the naked plasmid DNA deposit in the CS form in the absence of the supramolecular hybrid with height of approximately 2.0 nm.[25] Upon incubation with **1**, we notice that DNA has been condensed to form a spherical structure. As the ratio of **1**/DNA (*w*/*w*) increases from 16 to 24, the loose spheres become compact as evidenced by a height decrease from 50 nm (Figure 6b) to 20 nm (Supporting Information, Figure S9).[5,26] At the same time, Figure 6b clearly illustrates the DNA agglomerated with the SWCNT skeleton, which indicates that the supramolecular hybrid can be used as a spatially controllable DNA condensation system. The DNA aggregates on the nanometer scale as the discrete sphere along the individual SWCNT can explain the formation process of the sphere-like DNA bundles interlocking the individual tubes in the parallel lattice of SWCNTs.[10] This phenomenon can be explained by Johnson's theory about the molecular dynamics simulations of DNA adsorption on the positively charged SWCNT,[11b] that is, the phosphodiester groups of DNA have been attracted to the positively charged group on SWCNT surface. Considering the

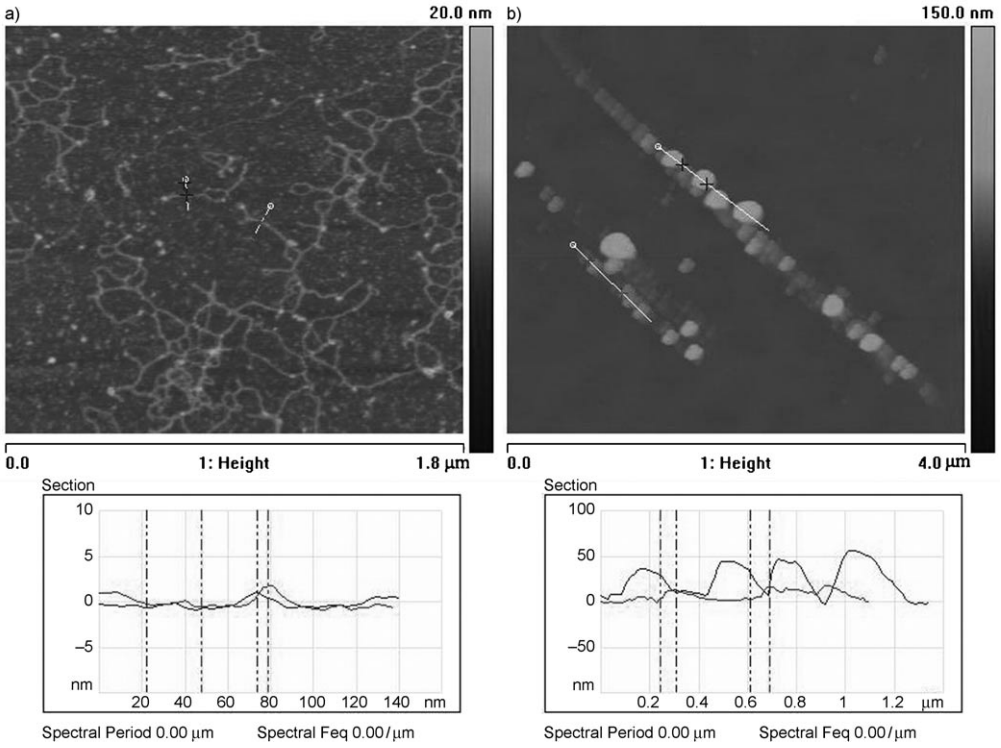

Figure 6. The AFM images of plasmid DNA, and its condensates induced by the supramolecular hybrid under the ambient condition. a) The naked pUC-19 plasmid DNA ([DNA] = 10 ng μL^{-1}); b) DNA condensates induced by supramolecular hybrid **1** ([DNA] = 10 ng μL^{-1}, [hybrid] = 160 ng μL^{-1}).

agarose gel electrophoresis analysis with ethidium bromide as an intercalating agent and the AFM image, we can deduce that **1** can be used to spatially control DNA condensation and as DNA-delivery system for gene therapy.[27]

The property of the **1**–DNA complex uptake by cells was also investigated with yeast (*Saccharomyces cerevisia*) cells with fluorescence microscopy. The supramolecular hybrid **1** and plasmid DNA were mixed and kept in the dark for 1 h, and then the mixture was added to the routinely cultured yeast cells for cell-uptake experiments under the fluorescence microscope. In the control experiments, yeast cells do not show luminescence in the presence of pUC-19 DNA and only show low luminescence in the presence of the supramolecular hybrid (Figure S10b).[28] In the experiment carried out with the **1**–DNA complex, however, we notice that nearly all of cells are luminescent under the fluorescence microscope (Figure S10d); this indicates a quite high DNA-delivery efficiency. These results demonstrate that the supramolecular hybrid based on SWCNT can be used as one efficient gene delivery system because the **1**–DNA complex can be uptaken by cells through the receptor-mediated endocytosis, and/or pinocytosis, and/or absorptive endocytosis processes.[2a] Owing to the reversibility of host–guest interaction between adamantane moiety and cyclodextrin, we also envision that this approach might improve gene expression activity within the cell.[29]

Conclusions

An aqueous supramolecular hybrid solution has been successfully obtained by supramolecular strategy based on SWCNT with the multiple supramolecular interactions, such as π–π stacking and host–guest interaction. The DNA condensation ability of the supramolecular system has been explored with agarose GEP analysis. The morphology features of hybrid–DNA complex have been investigated with AFM. We have noticed that the supramolecular hybrid can restrict the morphology of the hybrid–DNA complex, in other words, the supramolecular hybrid can be used as one spatially controllable DNA condensation system. Because the cell can respond to native topographical structures, the spatially controllable DNA condensation system is beneficial to nonviral gene delivery system. Furthermore, the reversibility of supramolecular host–guest interaction provides a potential approach for the release of DNA from the vector–DNA complex.

Experimental Section

Instrumental characterization: The UV/Vis/NIR spectra were recorded in a conventional quartz cuvette (light path 10 mm) on a Perkin–Elmer Lamda 900 UV/Vis/NIR spectrophotometer (Waltham, USA). High-resolution transmission electron microscopy (HRTEM) imaging was acquired with an FEI TECNAI G^2F20 (Hillsboro, USA) transmission electron microscope at an accelerating voltage of 200 kV. The sample was obtained from an aqueous solution (10 ng mL^{-1}) with a copper grid (3.00 mm, 200 mesh, coated with carbon film). The grid was dried under the ambient condition overnight. The atomic force microscopy (AFM) imaging was performed on a multimode Veeco Nano IIIa atomic force microscope (Camarillo, USA) in tapping mode to prevent damage to the samples under ambient conditions. A drop of sample solution was dropped onto newly cleaved mica and then air-dried overnight prior to AFM imaging. DNA condensation samples were incubated at 25 °C for 3 h in the dark before being dropped onto newly cleaved mica. X-ray photoelectron spectrum (XPS) was recorded by using an ESCALab 220i-XL electron spectrometer (VG Scientific, East Grinstead, UK) equipped with a monochromatic 300 W $Al_{K\alpha}$ radiation source ($h\nu = 1486.6$ eV), hybrid (magnetic/electrostatic) optics, and a multichannel plate and delay line detector. All XPS spectra were obtained by using an aperture slit width of 300 × 700 μm. The survey spectra were recorded with a pass energy of 160 eV, whereas high-resolution spectra were obtained with a pass energy of 40 eV. Raman spectra of solid samples were performed by using a Renishaw inVia Raman spectrometer (Gloucestershire, UK) equipped with a charge-coupled device (CCD) detector. The laser excitation was obtained by using a regular model laser operating at 633 nm with 5% output power and equipped with a 10× objective lens and a 25 μm slit. The laser beam was focused on the substrate (ca. 1 μm) with an exposure for 10 s. Wavenumber calibration was carried out by using the line at 520.5 cm^{-1} of the silicon wafer.

The agarose GEP analysis: A mixture of GEP sample (4 μL) and 6× loading buffer (1 μL) was added to a 1% (*w*/*v*) agarose gel containing 0.5 ng μL^{-1} ethidium bromide. Electrophoresis was carried out in the dark at RT with 0.5× TBE buffer (89 mM Tris/borate, 2 mM EDTA, pH 8.0) at 85 V for 1 h according to a standard protocol.[30] The DNA bands were visualized and photographed by a UV transilluminator and BioDoc-It imaging system (UVP, Upland, USA).

Optical and fluorescence microscopy: One drop of aqueous stained yeast cell solution was dropped on glass slips, and all optical and fluorescence microscopic images were performed on an OLYMPUS BX51 fluorescence microscope (Anaheim, USA) with a 100 W DC mercury lamp for excitation and a Mc MP5 color CCD camera for photo collection.

Materials: The SWCNT was commercially available from Carbon Nanotechnologies (Houston, USA) and purified according to a literature method.[31] (1-Adamantyl)ethanol (98%) and 1-pyrenebutyric acid (≥99.0%) were purchased from Aldrich. All other chemicals used were reagent grade unless otherwise noted. Ultrapure H_2O (>18.2 MΩ cm, 25 °C) was prepared by the Millipore-ELIX water-purification system. The pyrene derivative with a tethered adamantane group (Py-Ad) and $[Ru(phen)_2(\beta\text{-CD-hophen})]Cl_2$ complex (β-CD-RC) were prepared respectively according to the reported procedures.[5,13] The plasmid DNA pUC19 was purchased from Beijing Dingguo Biotechnology Co., Ltd (Beijing, China). The yeast (*S. cerevisia*) was obtained as a gift from the Department of Agronomy-Forestry Science, Huanghuai University.

Preparation of aqueous SWCNT–Py-Ad–β-CD-RC (1): Typically, a mixture of SWCNT, Py-Ad, and β-CD-RC (1 mg, 0.8 mg, 4 mg) was ground in an agate mortar and EtOH (1 mL) and ultrapure H_2O (2 mL) were added dropwise over the first 10 min. After further grinding for 3 h, the resultant black powder was then heated in a vacuum drying oven at 80 °C for 24 h. Finally, the dried black solid product was gently ground into a fine powder, which was then dispersed in 0.01 M NaOH (5 mL) with stirring for 4 h. The formed black suspension was further sonicated for 2 h, and then the pH was adjusted to 8.0. Centrifugation was used to remove insoluble material and gave aqueous **1** as the supernatant. The black SWCNT solution was subsequently dialyzed with ultrapure H_2O over a few days to ensure complete removal of excess β-CD-RC and Py-Ad. The obtained aqueous **1** was used in all experiments unless otherwise stated.

The dried solid sample was also obtained as a black powder by evaporating the aqueous supramolecular hybrid solution and then heated in a vacuum drying oven at 80 °C for 24 h.

Preparation of the sample for agarose gel electrophoresis (GEP) analysis: Plasmid DNA pUC19 was used as the model DNA for agarose gel electrophoresis analysis. A mixture of DNA (0.2 μg μL^{-1}) and aqueous **1**

in 1 mM EDTA/10 mM Tris buffer (pH 8.0) was incubated at RT in the dark for 1 h. All solutions were stored at 4 °C before use.

Preparation of yeast cell stain sample: The yeast (*S. cerevisia*) sample was dispersed in the YPD medium (2.0% yeast extract, 4% peptone, 2.0% glucose, 0.2% $(NH_4)_2SO_4$) and then cultured for 3 d at 35 °C. The obtained aqueous colony solutions, which were selected for cell staining, were incubated in the dark for 3 h at 35 °C with **1** (0.1 $g L^{-1}$) or supramolecular hybrid–DNA complex ([hybrid] = 0.1 $g L^{-1}$). Subsequently, these stained cells were collected by centrifugation to remove uncombined stain agent. The stained yeast cells were re-dispersed in ultrapure H_2O for further experiments.

Acknowledgements

We thank the 973 Program (2006CB932900, 2007CB808000), NNSFC (20932004, 20721062, and 20672025), and Tianjin Natural Science Foundation (07QTPTJC29600) for financial support.

[1] a) D. Ferber, *Science* **2001**, *294*, 1638–1642; b) M. A. Mintzer, E. E. Simanek, *Chem. Rev.* **2009**, *109*, 259–302; c) E. Check, *Nature* **2002**, *420*, 116–118.
[2] a) I. A. Khalil, K. Kogure, H. Akita, H. Harashima, *Pharmacol. Rev.* **2006**, *58*, 32–45; b) H. Lee, S. K. R. Williams, S. D. Allison, T. J. Anchordoquy, *Anal. Chem.* **2001**, *73*, 837–843; c) R. Tachibana, H. Harashima, Y. Shinohara, H. Kiwada, *Adv. Drug Delivery Rev.* **2001**, *52*, 219–226; d) P. Lehn, S. Fabrega, N. Oudrhiri, J. Navarro, *Adv. Drug Delivery Rev.* **1998**, *30*, 5–11.
[3] a) M. Köping-Höggård, K. M. Vårum, M. Issa, S. Danielsen, B. E. Christensen, B. T. Stokke, P. Artursson, *Gene Ther.* **2004**, *11*, 1441–1452; b) C. J. Bettinger, R. Langer, J. T. Borenstein, *Angew. Chem.* **2009**, *121*, 5512–5522; *Angew. Chem. Int. Ed.* **2009**, *48*, 5406–5415.
[4] a) A.-L. M. Le Ny, C. T. Lee, Jr., *J. Am. Chem. Soc.* **2006**, *128*, 6400–6408; b) A.-L. M. Le Ny, C. T. Lee, Jr., *Biophys. Chem.* **2009**, *142*, 76–83.
[5] Y. Liu, Y. Chen, Z.-Y. Duan, X.-Z. Feng, S. Hou, C. Wang, R. Wang, *ACS Nano* **2007**, *1*, 313–318.
[6] a) N. W. S. Kam, Z. Liu, H. Dai, *J. Am. Chem. Soc.* **2005**, *127*, 12492–12493; b) R. Singh, D. Pantarotto, L. Lacerda, G. Pastorin, C. Klumpp, M. Prato, A. Bianco, K. Kostarelos, *Proc. Natl. Acad. Sci. USA* **2006**, *103*, 3357–3362.
[7] a) J. Chen, S. Chen, X. Zhao, L. V. Kuznetsova, S. S. Wong, I. Ojima, *J. Am. Chem. Soc.* **2008**, *130*, 16778–16785; b) M. L. Becker, J. A. Fagan, N. D. Gallant, B. J. Bauer, V. Bajpai, E. K. Hobbie, S. H. Kacerda, K. B. Migler, J. P. Jakupiciak, *Adv. Mater.* **2007**, *19*, 939–945; c) M. Prato, K. Kostarelos, A. Blanco, *Acc. Chem. Res.* **2008**, *41*, 60–68.
[8] a) D. Pantarotto, R. Singh, D. McCarthy, M. Erhardt, J.-P. Briand, M. Prato, K. Kostarelos, A. Bianco, *Angew. Chem.* **2004**, *116*, 5354–5358; *Angew. Chem. Int. Ed.* **2004**, *43*, 5242–5246; b) R. Yang, X. Yang, Z. Zhang, Y. Zhang, S. Wang, Z. Cai, Y. Jia, Y. Ma, C. Zheng, Y. Lu, R. Roden, Y. Chen, *Gene Ther.* **2006**, *13*, 1714–1723; c) Z. Liu, M. Winters, M. Holodniy, H. Dai, *Angew. Chem.* **2007**, *119*, 2069–2073; *Angew. Chem. Int. Ed.* **2007**, *46*, 2023–2027; d) R. Krajcik, A. J ung, A. Hirsch, W. Neuhuber, O. Zolk, *Biochem. Biophys. Res. Commun.* **2008**, *369*, 595–602; e) M. Foldvari, M. Bagonluri, Nanomedicine, *NBM* **2008**, *4*, 173–182.
[9] Y. Liu, Z.-L. Yu, Y.-M. Zhang, D.-S. Guo, Y.-P. Liu, *J. Am. Chem. Soc.* **2008**, *130*, 10431–10439.
[10] a) R. Singh, D. Pantarotto, D. McCarthy, O. Chaloin, J. Hoebeke, C. D. Partidos, J.-P. Briand, M. Prato, A. Bianco, K. Kostarelos, *J. Am. Chem. Soc.* **2005**, *127*, 4388–4396; b) M. A. Herrero, F. M. Toma, K. T. Al-Jamal, K. Kostarelos, A. Bianco, T. D. Ros, F. Bano, L. Casalis, G. Scoles, M. Prato, *J. Am. Chem. Soc.* **2009**, *131*, 9843–9848.
[11] a) H. Lee, J. Mijoviæ, *Polymer* **2009**, *50*, 881–890; b) X. Zhao, J. K. Johnson, *J. Am. Chem. Soc.* **2007**, *129*, 10438–10445.
[12] a) N. Nakashima, Y. Tomonari, H. Murakami, K. Yoshinaga, *Chem. Lett.* **2002**, *31*, 638–639; b) T. Ogoshi, Y. Takashima, H. Yamaguchi, A. Harada, *J. Am. Chem. Soc.* **2007**, *129*, 4878–4879; c) W. Martin, W. Zhu, G. Krilov, *J. Phys. Chem. B* **2008**, *112*, 16076–16089; d) T. Ogoshi, M. Ikeya, T.-a. Yamagishi, Y. Nakamoto, A. Harada, *J. Phys. Chem. C* **2008**, *112*, 13079–13083; e) Y. K. Kang, O.-S. Lee, P. Deria, S. H. Kim, T.-H. Park, D. A. Bonnell, J. G. Saven, M. J. Therien, *Nano Lett.* **2009**, *9*, 1414–1418; f) J. Zou, S. I. Khondaker, Q. Huo, L. Zhai, *Adv. Funct. Mater.* **2009**, *19*, 479–483.
[13] S.-Z. Zu, X.-X. Sun, Y. Liu, B.-H. Han, *Chem. Asian J.* **2009**, *4*, 1562–1572.
[14] K. Liu, H. Fu, Y. Xie, L. Zhang, K. Pan, W. Zhou, *J. Phys. Chem. C* **2008**, *112*, 951–957.
[15] a) Y.-L. Zhao, L. Hu, G. Grüner, J. F. Stoddart, *J. Am. Chem. Soc.* **2008**, *130*, 16996–17003; b) K. A. Connors, *Chem. Rev.* **1997**, *97*, 1325–1357; c) Y. Liu, Y.-L. Zhao, Y. Chen, F. Ding, G.-S. Chen, *Bioconjugate Chem.* **2004**, *15*, 1236–1245.
[16] a) M. J. O'Connell, S. M. Bachilo, C. B. Huffman, V. C. Moore, M. S. Strano, E. H. Haroz, K. L. Bialon, P. J. Boul, W. H. Noon, C. Kittrell, J. P. Ma, R. H. Hauge, R. B. Weisman, R. E. Smalley, *Science* **2002**, *297*, 593–596; b) M. Zheng, A. Jagota, E. D. Semke, B. A. Diner, R. S. Mclean, S. R. Lustig, R. E. Richardson, N. G. Tassi, *Nat. Mater.* **2003**, *2*, 338–342; c) H. Paloniemi, T. Ritalo, T. Laiho, H. Like, N. Kocharova, K. Haapakka, F. Terzi, R. Seeber, J. Lukkari, *J. Phys. Chem. B* **2005**, *109*, 8634–8642; d) C. A. Dyke, J. M. Tour, *Chem. Eur. J.* **2004**, *10*, 812–817.
[17] a) N. Izard, D. Riehl, E. Anglaret, *Phys. Rev. B* **2005**, *71*, 195417; b) E. Nativ-Roth, R. Shvartzman-Cohen, C. Bounioux, M. Florent, D. Zhang, I. Szleifer, R. Yerushalmi-Rozen, *Macromolecules* **2007**, *40*, 3676–3685.
[18] A. Jorio, M. A. Pimenta, A. G. S. Filho, R. Saito, G. Dresselhaus, M. S. Dresselhaus, *New J. Phys.* **2003**, *5*, 139.1–139.17.
[19] R. Graupner, J. Abraham, A. Vencelová, T. Seyller, F. Hennrich, M. M. Kappes, A. Hirsch, L. Ley, *Phys. Chem. Chem. Phys.* **2003**, *5*, 5472–5476.
[20] a) C. D. Wagner, L. E. Davis, M. V. Zeller, J. A. Taylor, R. M. Raymond, L. H. Gale, *Surf. Interface Anal.* **1981**, *3*, 211–225; b) B. V. Crist, *Handbook of Monochromatic XPS SpectraThe Elements and Native Oxides*, Wiley, New York, **2000**.
[21] G. Wenz, B.-H. Han, A. Müller, *Chem. Rev.* **2006**, *106*, 782–817.
[22] Y. Yamasaki, Y. Teramoto, K. Yoshikawa, *Biophys. J.* **2001**, *80*, 2823–2832.
[23] H.-W. Zhang, L. Zhang, X. Sun, S. Diao, Z.-R. Zhang, *Biotechnol. Lett.* **2005**, *27*, 1701–1705.
[24] A. A. Stankus, M. A. Xapsos, C. J. Kolanko, H. M. Gerstenberg, W. F. Blakely, *Int. J. Radiat. Biol.* **1995**, *68*, 1–9.
[25] W.-X. Shi, R. G. Larson, *Nano Lett.* **2005**, *5*, 2476–2481.
[26] Z. Lin, C. Wang, X. Feng, M. Liu, J. Li, C. Bai, *Nucleic Acids Res.* **1998**, *26*, 3228–3234.
[27] B. Pitard, Soma, *Cell Mol. Gene.* **2002**, *27*, 5–15.
[28] A. Cass, A. Finkelstein, V. Krespi, *J. Gen. Physiol.* **1970**, *56*, 100–124.
[29] G. F. Walker, C. Fella, J. Pelisek, J. Fahrmeir, S. Boeckle, M. Ogris, E. Wagner, *Mol. Ther.* **2005**, *11*, 418–425.
[30] J. Sambrook, E. F. Fritsch, T. Manniatis, *Molecular Cloning: A Laboratory Manual*, 2nd ed., Cold Spring Harbor, New York.
[31] a) Y. Liu, A. Adronov, *Macromolecules* **2004**, *37*, 4755–4760; b) W. Zhao, C-V. Song, P. E. Pehrsson, *J. Am. Chem. Soc.* **2002**, *124*, 12418–12419.

Received: September 24, 2009
Published online: December 9, 2009

